Tipper, D. J., and Strominger, J. L. (1965), *Proc. Natl. Acad. Sci. U. S. 54*, 1133.
Tipper, D. J., and Strominger, J. L. (1968), *J. Biol. Chem. 243*, 3169.
Tipper, D. J., Strominger, J. L., and Ensign, J. C. (1967a), *Biochemistry 6*, 906.
Tipper, D. J., Strominger, J. L., and Ghuysen, J.-M. (1964), *Science 146*, 781.
Wise, E. M., and Park, J. T. (1965), *Proc. Natl. Acad. Sci. U. S. 54*, 75.

Specific Dissociation of Bacteriophage f_2 Protein to an 11S Component*

Peter O. Zelazo† and Rudy H. Haschemeyer

ABSTRACT: The ribonucleic acid bacteriophage f_2 was partially disaggregated by guanidine hydrochloride. Approximately one-half of the protein was obtained as an apparently homogeneous 11S component. The molecular weight of this stable degradative intermediate indicates the presence of 19 ± 1 polypeptide chains. The morphology of the particle was investigated by electron microscopic examination of negatively stained specimens.

Electron microscopy of the small RNA-containing bacteriophages often fails to provide detail sufficiently convincing to permit classification of these viruses into one of the icosahedral classes. Bacteriophage R_{17}, for example, has been classified as a 32 capsomer virus by Vasquez *et al.* (1966) while Klug and coworkers (1966) feel a 60 capsomer model is the correct one. Evaluation of the latter data must await publication of the details of their work. This difficulty in direct interpretation of electron micrographs may result from the partial collapse of the virus particle during electron microscopic preparation, the possible existence of additional protein subunits in an internal protein core, or the possibility that the virus is not, in fact, icosahedral. Even if these problems are not encountered, capsomer definition in electron micrographs diminishes rapidly as the size of the morphological subunit decreases. The visualization of extended apparent local symmetry resulting from superposition of capsomers negatively contrasted on the top and bottom of the particle then becomes a rare event and the likelihood of predominantly bottom stained particles probably diminishes as the size of the virus decreases.

Any of the above difficulties may be responsible for ambiguities in interpreting the structure of the spherical RNA bacteriophages and we have therefore used an alternate approach in which bacteriophage f_2 was dissociated by solvent perturbation to yield a product from which an apparently homogeneous preparation of virus subunits was obtained accounting for a majority of the original intact viral protein.

Experimental Section

Materials. Crystalline ribonuclease was obtained from Worthington Biochemical Corp., and G-HCl from Eastman Organic Chemicals. Ultraviolet-absorbing impurities were removed from the latter by twice applying the following procedure. Norit A (1.7 g) was added to 50 ml of the guanidine-coning buffer, shaken, and allowed to stand for 15 min. The Norit A was removed by vacuum filtration using Whatman No. 42 filter paper. Bacteriophage f_2 was obtained from an infected Hfr strain of *Escherichia coli* (AB312) and purified according to the method of Cooper and Zinder (1963).

Gel Electrophoresis. Polyacrylamide gel electrophoresis was conducted in Lucite tubes using a continuous buffer system (0.04 M Tris adjusted to pH 9.0 or 7.75 with HCl or 0.03 M sodium acetate adjusted to pH 5.0 with acetic acid). The gels were stained with Amido Black and destained by diffusion into 10% acetic acid.

Electron Microscopy. The negative staining procedures and electron microscopic methodology used in our laboratory has been previously described (Haschemeyer, 1968). Approximate particle dimensions were obtained from photographs containing admixed crystalline catalase according to the procedure described by Luftig (1967, 1968).

Zone Centrifugation. Sucrose gradient experiments were performed in a Spinco Model L2-65-B preparative ultracentrifuge using the SW27 Ti swinging-bucket rotor. A 7-ml layer of 20% sucrose in TKC[1] buffer was initially placed at the bottom of each cellulose nitrate tube, followed by a 5–20% linear sucrose gradient throughout the rest of the tube. All gradients were allowed to stand 4–8 hr before overlayering

* From the Department of Biochemistry, Cornell University Medical College, New York, New York 10021. *Received April 16, 1969.* Supported by grants from the U. S. Public Health Service (HE-11822) and the National Science Foundation (GB-7042).
† Supported by Public Health Predoctoral Fellowship No. 1-F1-GM-36,496.

[1] Abbreviation used is: TCK, 0.04 M Tris buffer–0.10 M KCl–0.005 M $CaCl_2$, titrated to pH 7.0 at 4° with HCl.

with 0.5 ml or less of sample. After centrifugation at 23,000 rpm for 40 hr, 0.9-ml fractions were collected from bottom-punctured tubes and analyzed for absorbancy in a Cary 15 spectrophotometer. These conditions were modified in order to prepare viral subunits free of any significant amount of RNA by including 4 M G-HCl in the sucrose gradient and centrifuging at 23,000 rpm for 40 hr.

Analytical Ultracentrifugation. Analytical ultracentrifugation was performed using the Spinco Model E analytical ultracentrifuge equipped with schlieren and interference optical systems and the photoelectric scanning system with multiplexer attachment. Certain modifications were introduced into the instrument to facilitate optical alignment and data taking. An externally rotatable mask assembly installed over the lower collimating lens (Bowers and Haschemeyer, 1969) was used to align the Rayleigh mask. Special masks were employed during photography of the interference data which effectively first masked a small vertical strip from each reference hole pattern. A second exposure made while masking the former area was then obtained with white light to provide a narrow strip of polychromatic fringes as an absolute reference for efficient plate alignment on the microcomparator. A Nikon Shadowgraph Model G microcomparator was utilized for measurement of the interference patterns, photographed on Kodak II-G spectroscopic plates.

Sedimentation velocity experiments were performed using double-sector cells with sapphire windows in an AN-D rotor and utilizing either the schlieren, ultraviolet, or interference optical systems. Optical alignment of the ultracentrifuge was conducted essentially as recommended by Gropper (1964), except that the optical system was focused on the $^2/_3$ plane of the cell (Yphantis, 1964).

Our earlier sedimentation equilibrium experiments were conducted in a manner which permitted maximal centrifugal redistribution while maintaining a slight macromolecular density gradient at the meniscus to avoid convective disturbances (induced by an unfortunate combination of line-voltage fluctuation, gearbox speed control, and drive-resonance vibration). Typically, protein concentration at the meniscus, C_m, was about 5% that of the original sample, C_o. Protein concentrations of 0.1–1.2 mg/ml were utilized with column heights of about 1.5 mm; 50 μl of sample and 10 μl of FC-43 were placed in the sample compartments of the standard Spinco six-channel centerpiece. On occasion, the FC-43 was omitted to confirm the absence of FC-43-induced aggregation. The reference channels were identically loaded with dialysate replacing sample. Time required to reach equilibrium was determined by comparing fringe shifts on time series photographs. After the equilibrium run, the cell was dismantled, cleaned, loaded with water, and accelerated to the equilibrium speed for obtaining base-line photographs.

Base-line-corrected Y displacement data (Yphantis, 1964) are converted into concentration difference data, Δc, by subtracting the most centripetal value from all the others. These data are then fitted to the equation

$$\ln (\Delta c + \Delta) = \frac{\sigma}{2}x^2 + I \qquad (1)$$

by choosing a value of Δ such that the standard deviation in $\ln (\Delta c + \Delta)$ of the calculated curve is a minimum. For a homogeneous ideal solute, the terms in eq 1 are interpreted as follows. Δ is the concentration at the first data point, $\sigma = M(1 - \bar{V}\rho)\omega^2/RT$ as defined by Yphantis (1964), and I is a constant of integration. For heterogeneous systems, the value of Δ chosen in this way approaches the true value of concentration at the first data point in the limit of fitting only points near the meniscus. In practice, this procedure introduces considerable error and for nearly homogeneous systems we prefer to obtain Δ from all the data points (a moving 11-point fit is also calculated to show any marked heterogeneity). The plot of $\ln (\Delta c + \Delta)$ *vs.* x^2 obtained in this manner deviates less from linearity than the true $\ln c$ *vs.* x^2 plot and is of questionable use for judging the degree of heterogeneity. However, the value of M computed from the slope quite closely approximates the z-average molecular weight, M_z, provided the principal component comprises 80% or more of the total protein. This conclusion is based on empirical results obtained by fitting eq 1 to calculated distributions of appropriate mixtures (W. Bowers and R. Haschemeyer, unpublished results). Alternatively, it may be seen that subtracting a small value from c in a gently curving $\ln c$ *vs.* x^2 plot to obtain the best straight line will result in a slope essentially identical with that at the column base of the true $\ln c$ *vs.* x^2 plot. Since at the speeds employed both c and dc/dx are small compared with the corresponding base value, M_w at the column base approximates M_z of the original solution (Yphantis, 1964).

Meniscus depletion equilibrium molecular weights were determined essentially as described by Yphantis (1964). These results were obtained after an electronic speed control was added to the Model E employed, which eliminated convective disturbances at the speeds used. An external loading multichannel centerpiece, as designed by A. Ansevin, D. Roark, and D. A. Yphantis (personal communication), was used for these studies. Base-line runs were made after cleaning, drying, and reloading the cell without dismantling. A 3-mm column height was used and the speed and concentration were chosen such that the fringe density at the bottom could always be resolved (40 fringes/mm in the cell) while the concentration midway in the column was within experimental error of zero (0.002 mm on the plate). The zero concentration level was chosen as the mean of points in the upper third of the cell, well within the range where the c *vs.* x plot was linear. Y displacements were calculated from the mean of three white fringes and data points were read every 0.050 mm on the plate.

Point-average values of the weight-average molecular weight, M_w, and number-average molecular weights, M_n, were calculated as described by Yphantis (1964).

An IBM 360–40 computer was used for the calculations and an on-line 1627 plotter provided graphical representation of selected data (W. Bowers and R. Haschemeyer, unpublished results).

Results

Purification of the 11S subunits. In early stages of this work, purified f_2 virus (at a concentration of about 12 mg/ml) was degraded at pH 7.0 in TKC buffer by diluting into G-HCl containing buffers to various final guanidine concentrations from 1.0 to 4.0 M. Sedimentation velocity studies using the schlieren optical system demonstrated that in 4.0 M G-HCl most of the viral protein had a sedimentation coefficient, $s_{20,w}$ of 11 S. These conditions were chosen to provide material for subsequent purification. The virus solutions con-

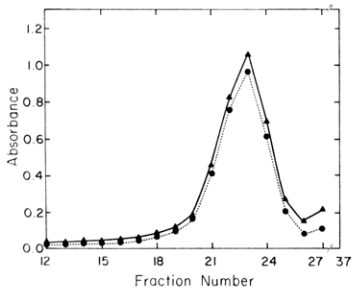

FIGURE 1: Sucrose gradient centrifugation of the 11 S component. The solid line and dotted line represent absorbance at 280 and 260 mμ, respectively. Fraction numbers up to 14 were at the base-line level and those above 37 rose to off-scale levels due to the presence of degraded RNA. Other details are given in the text.

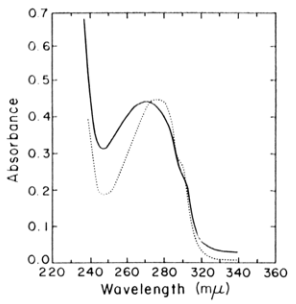

FIGURE 2: Ultraviolet spectra in TKC buffer of the 11S component isolated from sucrose gradients run in the presence (broken line) and absence (solid line) of 4 M G-HCl.

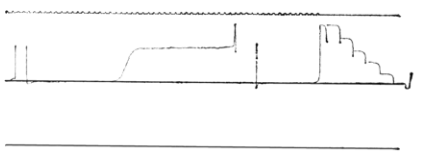

FIGURE 3: Sedimentation velocity of the 11S component. The photoelectric scanner pattern was taken 21 min after reaching a speed of 59,780 rpm. The experiment was conducted at 24° in TKC buffer.

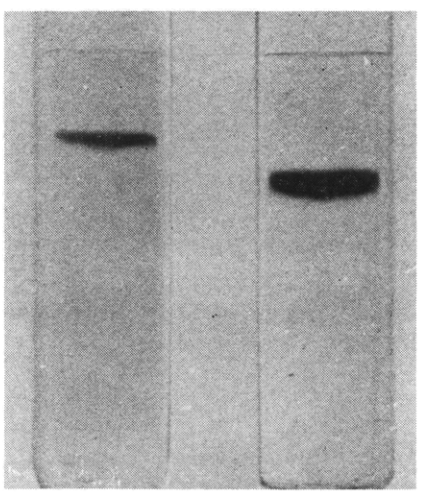

FIGURE 4: Gel electrophoresis of the 11S particle at pH 7.75. The 6% gel on the left was run with 8 μg of protein. The 4% gel on the right was run with 32 μg of protein. Electrophoresis was carried out at 120 V for 2 hr in 0.04 M Tris buffer.

taining 4.0 M G-HCl were dialyzed extensively against TKC buffer in the cold to remove G-HCl and were then incubated with 35 μg of ribonuclease/ml for 1.5 hr at 25°. Any precipitate was removed from solution by low-speed centrifugation at 7000 rpm in a Spinco Model L centrifuge using the 40 rotor for 10 min at 4°. The 11S component was separated from the mixture on a sucrose gradient and fractions containing the 11S component (Figure 1) were subjected to solvent exchange with TKC buffer and concentrated to 1–2 mg/ml in a small volume ultrafiltration cell (Bowers and Haschemeyer, 1968).

Material isolated in this fashion contains about 3% RNA as calculated from its ultraviolet spectrum (Figure 2) (Layne, 1957). These low molecular weight oligonucleotides could be removed by purification on a sucrose gradient containing 4.0 M G-HCl throughout. The 11S component isolated in this fashion has a typical protein spectrum (Figure 2).

The yield of 11S component was determined by refractive index measurement. Purified virus (12 mg/ml) in TKC buffer was identically diluted into both TKC buffer alone and into TKC buffer containing 4.0 M G-HCl. Interference photographs of the undegraded virus during sedimentation velocity at 25,980 rpm were used to obtain the concentration, in fringes, across the virus boundary. This was corrected for radial dilution and the concentration of protein calculated from the known protein content of the RNA bacteriophages (Gussin *et al.*, 1966) and the refractive increments of RNA and f_2 protein (assuming "typical" values of 0.194 and 0.185 ml per g, respectively). The degraded solution was dialyzed to remove G-HCl and treated with 35 μg/ml of RNase for 1.5 hr at 25°. The resulting dilution was determined volumetrically. The concentration of protein, in fringes, was then determined by sedimentation velocity at 42,000 rpm as described above for intact virus. Comparison of the two values showed that 51% of the protein of the original virus was contained in the 11S boundary.

The purified 11S component migrated as a single sharp boundary in sedimentation velocity experiments (Figure 3) and showed a single band on gel electrophoresis at pH 5.0, 7.75 (Figure 4), and 9.0.

Molecular Weight Determinations. A typical sedimentation equilibrium result obtained with the Yphantis method is shown in Figure 5. A summary of all molecular weight determinations is presented in Table I. The near linearity of $d \ln c/dx^2$ indicates that a contamination of more than 5% with species differing in molecular weight by a factor of 2 or more (*e.g.*, aggregates) is unlikely. This is well within the limit where the Δc calculations give a reliable estimate for M_z if solute concentration at the meniscus is 0.1 C_0 or less. Point-average values of M_n and M_w showed upward curvature consistent with 5% dimer in three of the Yphantis runs and were linear and equal in the other three. We are not certain if these differences reflect experimental error or represent minor but real differences in the state of aggregation of the sample used. No significant change in molecular weights were detected in runs where the FC-43 was deleted.

The known molecular weight of f_2 coat protein (Konigsberg, 1966; Konigsberg *et al.*, 1966; Weber and Konigsberg, 1967) may be combined with the measured molecular weight of 270,000 ± 6,000 to conclude that the 11S component contains about 19 polypeptide chains. The major uncertainties reside in calculating the partial specific volume from amino acid composition data (Weber and Konigsberg, 1967) and the possible

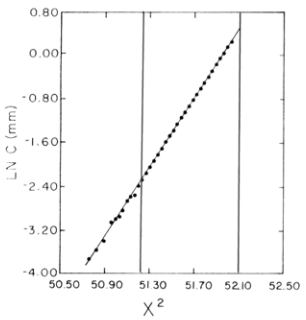

FIGURE 5: Sedimentation equilibrium of the 11S component (meniscus depletion method of Yphantis (1964)). The vertical line on the left represents the position of the first point included in the least-square calculation, corresponding to a displacement of 0.100 mm. The second vertical line shows the position of the solution bottom. The point at this x^2 position is the intercept calculated from the least-square line. Concentration is reported as millimeter displacement on the plate (0.290 mm is equivalent to one fringe). The data were obtained at 14,000 rpm at a protein concentration of 0.12 mg/ml in TKC buffer at 7°.

existence of some undetectable aggregation.

Electron Microscopy. The 11S component characteristically has an ellipsoidal shape when negatively stained with uranyl oxalate (Figure 6), sodium phosphotungstate, or uranyl acetate. Subunit detail remains largely obscured in most particles, but an open center penetrable by stain is clearly seen. Occasional particles have a morphology better described as two parallel bars and some are nearly spherical in shape. Average dimensions of the predominating ellipsoidal shape are 50 × 103 Å.

Dialysis of the 11S component against sodium acetate buffer (0.1 M) at pH 4.0 in the cold, followed by dilution with water just prior to negative staining with uranyl acetate (0.2%, pH 4), induced oriented aggregation into small two-dimensional "crystallites" as shown in Figure 7. Although oriented areas seldom were large, a majority of particles participated in the interparticle bonding whereby each appears to be in closest proximity to four nearest neighbors. The compressed hexagonal appearance in the uranyl acetate stained crystallites of the otherwise ellipsoidal appearing 11S particles may be due to a staining artifact induced by the ordered packing of molecules.

A similarly shaped particle is observed in another type of two-dimensional array induced by formaldehyde fixation at pH 4 prior to staining as above (Figure 8). The predominant aggregation is now end to end along the major dimension of the particle. Side-by-side aggregation occurs to a lesser extent, and each particle ultimately appears to be bounded by six nearest neighbors.

TABLE I: Sedimentation Equilibrium Molecular Weight Determinations of the 11S Component.

Meniscus Depletion Method	*C* Method
275,000	272,000
270,000	275,000
274,000	279,000
263,000	271,000
273,000	272,000
261,000	261,000
	264,000
Mean 270,000 ± 6,000	

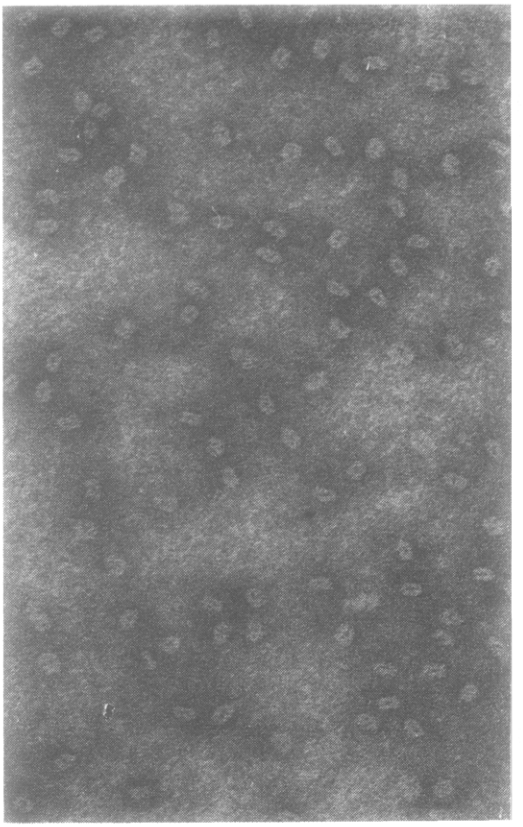

FIGURE 6: The 11S component negatively contrasted with uranyl oxalate at pH 6.8. Dimensions of the predominant ellipsoidal form are about 103 × 50 Å.

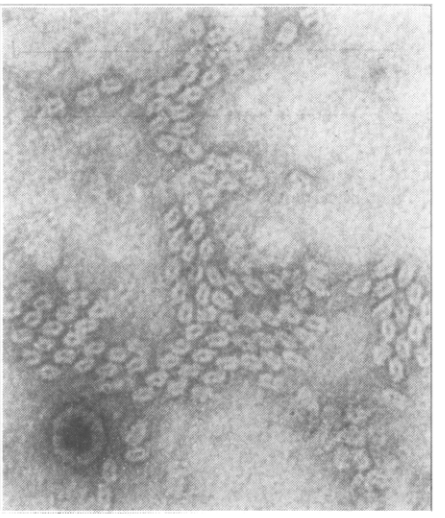

FIGURE 7: The 11S component negatively stained with uranyl acetate at pH 4.0, showing the low pH-induced aggregation. An intact virus particle is included for perspective.

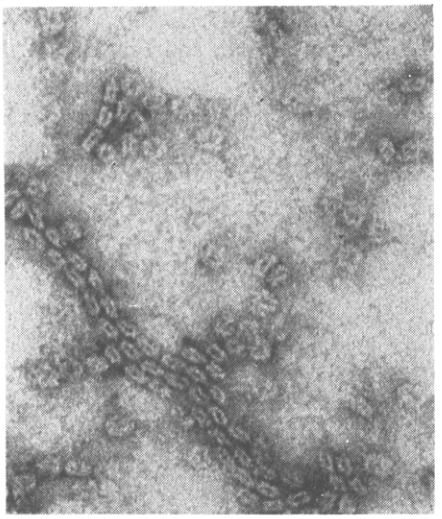

FIGURE 8: Negatively contrasted 11S particles showing formaldehyde-induced association.

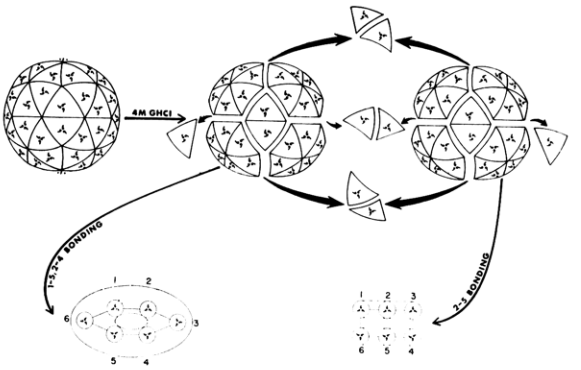

FIGURE 9: Proposed mode of degradation of the 60 capsomer model. Details are described in the text.

Discussion

Bacteriophage f_2 is composed essentially of only one type of polypeptide chain since the "A protein" (Roberts and Argetsinger Steitz, 1967; Argetsinger Steitz, 1968) is quantitatively insignificant in this study. If the virus is icosahedral, it must contain 180 structural units to be compatible with physical and chemical data (*e.g.*, see the reviews by Gussin *et al.* (1966) and Kaper (1968) and references cited therein). The characterization of the 11S component presented here is incompatible with a species representing dissociated capsomers of the 32, 60, or 90 capsomer model (Casper and Klug, 1962; Finch and Holmes, 1967). We have therefore considered the possibility that the 11S particle might represent a cluster of capsomers arising from preferential dissociation or solubility of quasi-equivalent structures.

No method of dissociating the 32 or 90 capsomer model of 180 subunits was found which could reasonably give rise to a major product closely resembling the 11S component, but compatability with a 180 subunit–60 capsomer model can be demonstrated with a minimum of assumptions. The manner in which the 11S component may be derived from the 60 capsomer model is shown schematically in Figure 9. The spherical model to the left of the diagram represents the distribution of the 180 polypeptide chains into 60 trimer clusters. The degradation of the 60 capsomer model is visualized as a dissociation into the 8 hexamers and 12 monomers indicated in the diagram (both halves shown).

The isolated hexamers would be expected to have six trimers located equidistant from a sixfold rotational axis. The 11S component with geometry compatible with the electron micrographs can then be formed if the capsomers labeled 1 to 6 are given sufficient angular freedom to permit formation of additional one to five and two to four bonding sets (the occasional rectangular particles observed may reflect the additional possibility of forming two to five contacts). It is further necessary to postulate that alternate products of dissociation (*e.g.*, pentameric clusters) and trimers *per se* were not obtained because of limited solubility.

We do not necessarily advocate acceptance of the above model and have presented it primarily to provide one alternative to the more direct literal interpretation of the properties of the 11S particle, since the latter would require abandoning an icosahedral model for bacteriophage f_2 altogether.

Acknowledgment

We thank Professor Roy Swan and the Department of Anatomy for generously providing time on their Philips 200 electron microscope and the Biomathematics Computing Center for making their facilities available to us. Mr. Vincent Nolin's care in maintaining the electron microscope and the technical assistance of Miss Celeste Targum is most appreciated. We thank Dr. Daniel Wellner for valuable discussions, Dr. Steven Cooper for his help during the early stages of the work, and Mr. William Bowers for his role in the development of procedures utilized for molecular weight determinations.

References

Argetsinger Steitz, J. E. (1968), *J. Mol. Biol. 33*, 923, 937.

Bowers, W., and Haschemeyer, R. (1968), *Anal. Biochem. 25*, 549.

Bowers, W., and Haschemeyer, R. (1969), *Anal. Biochem.* (in press).

Caspar, D. L. D., and Klug, A. (1962), *Cold Spring Harbor Symp. Quant. Biol. 25*, 1.

Cooper, S., and Zinder, N. (1963), *Virology 20*, 605.

Finch, J. T., and Holmes, K. C. (1967), *in* Methods in Virology, Vol. III, Maramorosch, K., and Koprowski, H., Ed., New York, N. Y., Academic, p 351.

Gropper, L. (1964), *Anal. Biochem. 7*, 401.

Gussin, G. N., Capecchi, M. R., Adams, J. M., Argetsinger Steitz, J. E., Tooze, J., Weber, K., and Watson, J. D. (1966), *Cold Spring Harbor Symp. Quant. Biol. 31*, 25.

Haschemeyer, R. (1968), *Trans. N. Y. Acad. Sci. 30*, 875.

Kaper, J. M. (1968), *in* Molecular Basis of Virology, Fraenkel-Conrat, H., Ed., New York, N. Y., Reinhold, p 1.

Klug, A., Finch, J. T., Leberman, R., and Longley, W. (1966), *in* Ciba Foundation Symposium, Principles of Biomolecular Organization, Wolstenholme, G. E. W., and O'Connor, M., Ed., Boston, Mass., Little Brown, p 158.

Konigsberg, W. (1966), *J. Biol. Chem. 241*, 4534.

Konigsberg, W., Weber, K., Notani, G., and Zinder, N. (1966), *J. Biol. Chem. 241*, 2579.
Layne, E. (1957), *Methods Enzymol. 3*, 447.
Luftig, R. (1967), *J. Ultrastruct. Res. 20*, 91.
Luftig, R. (1968), *J. Ultrastruct. Res. 23*, 178.
Roberts, J. W., and Argetsinger Steitz, J. E. (1967), *Proc. Natl. Acad. Sci. U. S. 58*, 1417.
Vasquez, C., Granboulan, N., and Franklin, R. M. (1966), *J. Bacteriol. 92*, 1779.
Weber, K., and Konigsberg, W. (1967), *J. Biol. Chem. 242*, 3563.
Yphantis, D. A. (1964), *Biochemistry 3*, 297.

Solid-Phase Synthesis and Some Pharmacological Properties of [8-Phenylalanine]-Oxytocin*

J. W. M. Baxter, M. Manning,† and W. H. Sawyer

ABSTRACT: In an attempt to establish the identity of a principle designated as EOP I (elasmobranch oxytocin-like principle I), which has been isolated from the pituitary gland of the spiny dogfish (*Squalus acanthias*), [8-phenylalanine]-oxytocin has been synthesized and tested for some of the pharmacological activities characteristic of the neurohypophysial hormones. The synthesis was accomplished by means of the Merrifield solid-phase method as employed for the synthesis of oxytocin and glumitocin. After purification by gel filtration on Sephadex G-15, the product was obtained in 38% over-all yield.

Bioassays yielded the following activities with their 95% confidence limits: rat uterus (no Mg^{2+}), 108 (100–117) units/mg; rat uterus (+Mg^{2+}), 366 (332–406) units/mg; fowl vasodepressor, 191 (170–214) units/mg; rabbit milk ejection, 341 (316–368) units/mg; rat vasopressor, 0.97 (0.90–1.04) units/mg; rat antidiuretic, 1.16 (0.92–1.46) units/mg; and frog bladder activity, 1700 (1240–2360) units/mg. A comparison of these properties with those obtained for EOP I indicates that the latter is not [8-phenylalanine]-oxytocin.

The structures of seven naturally occurring neurohypophysial hormones are known (Table I). In these principles five different amino acids occupy position 8 of the common cyclic octapeptide structure, and two in each of positions 3 and 4.

A principle termed EOP I[1] has been isolated from the pituitary gland of the spiny dogfish (*Squalus ascanthias*) with biological properties similar to those of oxytocin analogs containing a neutral amino acid at position 8 (Sawyer, 1967), but differing in its pharmacological properties from any of the known neurohypophysial hormones or synthetic analogs with which it has been compared. So far, it has not been possible to obtain sufficient quantities of pure material to enable characterization studies to be carried out in the usual manner, *i.e.*, through amino acid analysis and subsequent sequence studies. In an attempt to elucidate the structure of EOP I, it was considered worthwhile to utilize knowledge of its physical and pharmacological properties with that of the evolutionary pattern of the neurohypophysial hormones, to predict what its structure might be and to test this prediction by the synthetic approach. Since evolutionary changes have occurred most frequently at position 8, it was thought possible that EOP I might be an analog of oxytocin containing yet another amino acid in this position. EOP I has been shown to have a slightly higher R_F value than oxytocin on a partition column (Sawyer, 1967). Thus it was reasoned that an amino acid possessing similar lipophylic properties to those of the leucine residue at position 8 in oxytocin might be present in position 8 of EOP I and it might indeed be phenylalanine. Because of this reasoning and also because of our general interest in structure–activity relationships of the neurohypophysial hormones we synthesized [8-phenylalanine]-oxytocin and compared its pharmacological properties with those of EOP I.

The key intermediate required for the synthesis of [8-phenylalanine]-oxytocin was the protected nonapeptide *N*-benzyloxycarbonyl-*S*-benzyl-L-cysteinyl-*O*-benzyl-L-tyrosyl-L-isoleucyl-L-glutaminyl-L-asparaginyl-*S*-benzyl-L-cysteinyl-L-prolyl-L-phenylalanylglycinamide. This protected nonapeptide intermediate was synthesized by the solid-phase method (Merrifield, 1963, 1964) following essentially the procedure outlined in the synthesis of oxytocin (Manning, 1968) and of glumitocin (Manning *et al.*, 1968a). BOC-glycine was esterified to the chloromethylcopolystyrene–2% divinylbenzene resin and the stepwise synthesis was carried through eight cycles of deprotection, neutralization, and coupling with the appropriate BOC-amino acids to give the fully protected peptide-resin: *N*-benzyloxycarbonyl-*S*-benzyl-L-cysteinyl-*O*-ben-

* From the Department of Biochemistry, McGill University, Montreal, Quebec, Canada, and the Department of Pharmacology, College of Physicians and Surgeons of Columbia University, New York, New York 10032. *Received May 22, 1969.* This work was supported in part by a Studentship (to J. W. M. B.) and an Operating grant (to M. M.) from the Medical Research Council of Canada, a National Science Foundation Grant No. GB-4932X and a General Research Support Grant to Columbia University from the National Institutes of Health.

† To whom inquiries should be directed at the Department of Biochemistry, Medical College of Ohio, Toledo, Ohio 43614.

[1] Abbreviation used is: EOP I, elasmobranch oxytocin-like principle I.